Synchronization between different motifs*

Li Ying(李 莹)[a)†] and Liu Zeng-Rong(刘曾荣)[b)]

[a)] College of Information Technology, Shanghai Ocean University, Shanghai 201306, China
[b)] Institute of Systems Biology, Shanghai University, Shanghai 200444, China

(Received 6 February 2010; revised manuscript received 5 July 2010)

In this paper, we study the synchronization between different motifs. First, the synchronization between two networks with different topology structures and different dynamical behaviours is studied. With the open-plus-closed-loop(OPCL) method, conditions for two different networks to realize synchronization are given. Then based on the theoretical results achieved, the synchronization between different motifs is studied, which verifies the effectiveness and feasibility of the synchronization scheme.

Keywords: OPCL method, motif, synchronization
PACC: 0500, 0547

1. Introduction

Up to now, complex network has become a common topological structure to describe many real systems.[1] Complex networks are often modular in nature, collaborating with groups of individual nodes to carry out some specific functions. This has led researchers to look for patterns on the basis of statistical significance. To determine statistical significance, one compares the network to an ensemble of randomized networks. The randomized networks are networks with the same characteristics as those of the real network, (e.g., the same numbers of nodes and edges as those of the real work), where the connections between nodes and edges are made at random. Small subgraphs that occur in the real network significantly more often than in randomized networks are called network motifs.[2,3] Motifs are suggested to be elementary building blocks that carry out key functions in the network, and they have been found in networks of biochemistry, neurobiology, ecology, engineering, and so on.[3] Many kinds of researches have been carried out thereby become an important aspect of network research. Motifs shared by different networks are distinct from each other; besides, they can determine a broad class of networks, each with specific type of elementary structure.[3] Motifs are important because they reflect the underlying processes that generate each type of network to a degree.

The reasons why network motifs occur more often in a special network is still poorly understood. Up to now, some researches have been carried out from a dynamical point of view for the question.[4] In our previous paper,[5] we studied the dynamical property of genetic regulatory network motifs. We obtained the conclusion that network motif was a basic and stable structure and the combinations of motifs could exhibit complicated properties. Moreno *et al.*[6] studied the fitness for synchronization of network motifs. With the Kuramoto model, it was concluded that the higher the interconnection between motif constituents is, the lower the synchronization threshold is. The synchronization threshold was also in agreement with the natural conservation ratio(NCR). The NCR is a quantity proposed in Ref. [7], to measure the conservation of a given motif in evolution across species. In Ref. [8], the authors proposed an analytic method to measure the stability of the synchronous state(SSS) displayed by motifs. They observed a general increase in SSS as the number of the edges in motif increased, which was in accordance with the decrease of the synchronization threshold in Ref. [6]. The SSS's were also in good accordance with the NCR. These accordances of the synchronization threshold and the SSS with the NCR indicate that motifs are preserved during evolution with a higher probability.

Considering that motifs occur very often in complex networks, we can take motifs as basic elements to synthesize a complex network. Numerical simulation of network synchronization shows that the synchronization of a whole network is usually achieved

*Project supported by the Doctoral Research Fund of Shanghai Ocean University, the Science Foundation for the University Excellent Youth Scholars of Shanghai, and the National Natural Science Foundation of China (Grant No. 10832006).
†Corresponding author. E-mail: leeliying@163.com
© 2010 Chinese Physical Society and IOP Publishing Ltd

through the cluster synchronization by extending cluster gradually to the whole network. One possible process is probably realized by motifs' synchronization. So it is important to study the synchronization between motifs. However, motifs in different networks are different, and different motifs in the same complex network have different functions.[9,10] It is a natural question whether the synchronization between different motifs can be achieved. Take society networks as examples. Before a decision-making, there may be many different viewpoints from different groups. Among all these groups, there is generally one influential group which plays a crucial role in decision making. First, the influential group has to achieve accordant points, which is regarded as the 'inner synchronization' as it is a collective behaviour within a network; then the other groups are influenced and achieve the same points with the influential group, which is regarded as the 'outer synchronization' which illustrates the synchronization between two or more complex networks. Thus the decision-making is obtained. If we take motifs as the basic elements, it is a problem about the synchronization between different motifs.

This problem can be reduced into the synchronization between different networks with both different topology structures and different dynamical behaviours. Although there are many studies on the synchronization of nodes in all kinds of networks,[11−13] few of them focus on the synchronization between networks.[14] Recent work of synchronization between two completely the same networks were carried out in Ref.[15], but no researches were carried out to solve the problem mentioned above. In the present paper, we will give some discussion on this question and prove that the synchronization between different networks can be obtained with the help of OPCL control method. Then we apply our theoretical results to the synchronization between different motifs. Numerical simulation verifies the theoretical results.

2. Synchronization between two different networks

In 1995, Jackson and Grousu[16] offered a control method of open-plus-closed-loop (OPCL) for the first time. Consider a general system

$$\frac{\mathrm{d}x}{\mathrm{d}t} = f(x), \qquad x \in R^n. \tag{1}$$

The original OPCL method offers a driving for system (1) to achieve a desired 'goal' behaviour, $g(t) \in R^n$. The driving has the following form:

$$D(x, g) = D_1(g) + D_2(x, g), \tag{2}$$

where $D_1(g) = \mathrm{d}g/\mathrm{d}t - f(g)$ is an open-loop driving, $D_2(x, g) = (\boldsymbol{H} - \partial f(g)/\partial g)(x - g)$ is a closed-loop(feedback) one, and $\boldsymbol{H}$ is an arbitrary constant Hurwitz matrix. The driven system

$$\frac{\mathrm{d}x}{\mathrm{d}t} = f(x) + D(x, g) \tag{3}$$

has an asymptotic behaviour $x(t) \to g(t)$, if $\|x(0) - g(0)\|$ is small enough.[16,17]

The matrix $\boldsymbol{H}$ can be chosen in such a way that $D_2(x, g)$ is as simple as possible. When $(\partial f(g)/\partial g)_{ik}$ is constant, we can choose $H_{ik} = (\partial f(g)/\partial g)_{ik}$ and $(D_2(x, g))_{ik} = 0$, otherwise we can introduce one or several parameters into the matrix $\boldsymbol{H}$ to guarantee that matrix $\boldsymbol{H}$ is a Hurwitz matrix.[18] From this we can conclude that $D_2(x, g)$ will be simpler if $f(g)$ has fewer nonlinear terms.

Now we consider the synchronization between two different networks X and Y. These two networks may be undirected or directed, and the dynamic behaviours of nodes in different networks are quite different. With the OPCL control method, the equations of motion read

$$\begin{aligned} \dot{\boldsymbol{x}}_i(t) &= F(\boldsymbol{x}_i(t)) + \mu \sum_{k=1}^{N_1} a_{ik} \boldsymbol{\Gamma}_1 x_k(t), \\ & \qquad i = 1, 2, \ldots, N_1, \end{aligned} \tag{4}$$

$$\begin{aligned} \dot{\boldsymbol{y}}_i(t) &= G(\boldsymbol{y}_i(t)) + \varepsilon \sum_{k=N_1+1}^{N_1+N_2} b_{ik} \boldsymbol{\Gamma} y_k(t) \\ &\quad + D(\boldsymbol{y}_i(t), \boldsymbol{x}_i(t)), \\ & i = N_1 + 1, \ldots, N_1 + N_2, \ j \in \{1, 2, \ldots, N_1\} \end{aligned} \tag{5}$$

with

$$\begin{aligned} D(\boldsymbol{y}_i, \boldsymbol{x}_i) &= D_1(\boldsymbol{x}_i) + D_2(\boldsymbol{y}_i, \boldsymbol{x}_i) \\ &= F(\boldsymbol{x}_i) - G(\boldsymbol{x}_i) \\ &\quad + (\boldsymbol{H} - \partial G(\boldsymbol{x}_i)/\partial \boldsymbol{x}_i)(\boldsymbol{y}_i - \boldsymbol{x}_i), \end{aligned} \tag{6}$$

where $\boldsymbol{x}_i = (x_i^1, \ldots, x_i^n)^\top \in R^n$ and $\boldsymbol{y}_i = (y_i^1, \ldots, y_i^n)^\top \in R^n$ are n-vectors containing the coordinates of the ith node in networks X and Y, respectively; N_1 and N_2 are numbers of nodes in X and Y networks respectively; $F : R^n \to R^n$ and $G : R^n \to R^n$ are continuously differentiable functions which determine the dynamical behaviours of

the nodes without coupling; $\mu > 0$ and $\varepsilon > 0$ are coupling strengths; $\boldsymbol{\Gamma}_1$ and $\boldsymbol{\Gamma}$ are matrices that are determined by the variables with which the nodes are coupled. For clarity, we shall consider the diagonal matrices $\boldsymbol{\Gamma}_1 = \mathrm{diag}(\overbrace{1,1,\ldots,1}^{s_1},0,\ldots,0)_{n\times n}$ and $\boldsymbol{\Gamma} = \mathrm{diag}(\overbrace{1,1,\ldots,1}^{s},0,\ldots,0)_{n\times n}$. Let $\boldsymbol{A} = (a_{ij})_{N_1\times N_1}$ and $\boldsymbol{B} = (b_{ij})_{N_2\times N_2}$ be respectively the inner connectivity matrices of networks X and Y, which are both irreducible, and assume them to be symmetric or asymmetric and to satisfy zero row-sums. The entries $a_{ij}(b_{ij})$ are defined as follows: $a_{ij} = 1(b_{ij} = 1)$, if there is a connection from node i to node j, $i \neq j$; otherwise, $a_{ij} = 0(b_{ij} = 0)$, $i \neq j$; $a_{ii} = -\sum_{j=1,j\neq i}^{N_1} a_{ij}(b_{ii} = -\sum_{j=N_1+1,j\neq i}^{N_1+N_2} b_{ij})$.

As far as the synchronization of driving network (4) is concerned, many researches have been carried out.[19−23] We say network X to achieve synchronization if $\lim_{t\to+\infty}\|x_j - x_i\| = 0,\ i,\ j = 1,\ldots,N_1$. The synchronous state of system (4) is defined by the linear invariant manifold $M = \{x_1 = x_2 = \cdots = x_{N_1}\}$. This invariant manifold has a dimension $n\times(N_1-1)$ and is often called the synchronization manifold. For the conditions of the nodes for system (4) to achieve synchronization, one can consult Ref. [21] for undirected networks and Ref. [22] for directed networks with node balance.

From the previous papers, we know that the synchronous state of network X can be obtained, no matter whether the network X is directed or undirected. The dynamics of the synchronous state can be described by the following system:

$$\dot{x}(t) = F(x(t)). \tag{7}$$

Under the precondition that network X reaches synchronization, system (7) can be regarded as a driving system, and the corresponding response network (5) can be described by the following system:

$$\begin{aligned}\dot{y}_i(t) &= G(y_i(t)) + \varepsilon\sum_{k=N_1+1}^{N_1+N_2} b_{ik}\boldsymbol{\Gamma}y_k(t) + F(x(t))\\ &\quad -G(x(t)) + (\boldsymbol{H} - \partial G(x)/\partial x)(\boldsymbol{y}_i(t) - \boldsymbol{x}(t)).\end{aligned} \tag{8}$$

Defining the following errors

$$\delta_i(t) = \boldsymbol{y}_i(t) - \boldsymbol{x}(t), \quad i = N_1+1,\ldots,N_1+N_2$$

and noting $\sum_{k=N_1+1}^{N_1+N_2} b_{ik} = 0$, one obtains the linearized error system around x by taking the Taylar expansion $G(y_i) = G(x+\delta_i) = G(x)+(\partial G(x)/\partial x)\delta_i+\ldots$ as follows:

$$\begin{aligned}\dot{\delta}_i &= G(x) + (\partial G(x)/\partial x)\delta_i + \varepsilon\sum_{k=N_1+1}^{N_1+N_2} b_{ik}\boldsymbol{\Gamma}y_k\\ &\quad +F(x) - G(x) + (\boldsymbol{H} - \partial G(x)/\partial x)\delta_i - F(x)\\ &= \boldsymbol{H}\delta_i + \varepsilon\sum_{k=N_1+1}^{N_1+N_2} b_{ik}\boldsymbol{\Gamma}\delta_k.\end{aligned} \tag{9}$$

Letting $\boldsymbol{\delta} = [\delta_{N_1+1}, \delta_{N_2+2}, \ldots, \delta_{N_1+N_2}]$, one obtains the vector form of system (9)

$$\dot{\boldsymbol{\delta}} = \boldsymbol{H}\boldsymbol{\delta} + \varepsilon\boldsymbol{\Gamma}\boldsymbol{\delta}B^{\top}. \tag{10}$$

The stabilities of the synchronous solutions of Eqs. (7) and (8) are determined by the variational equation of Eq. (10). For matrix $\boldsymbol{B}$, there exists an invertible matrix $\boldsymbol{P}$ of the generalized eigenvectors of $\boldsymbol{B}$, which transforms $\boldsymbol{B}$ into Jordan canonical form as $\boldsymbol{P}^{-1}\boldsymbol{B}\boldsymbol{P} = \boldsymbol{J}$, where

$$\boldsymbol{J} = \begin{pmatrix} 0 & & & \\ & L_1 & & \\ & & \ddots & \\ & & & L_d \end{pmatrix},$$

$$\boldsymbol{L}_j = \begin{pmatrix} \lambda_j & & & \\ 1 & \lambda_j & & \\ & \ddots & \ddots & \\ & & 1 & \lambda_j \end{pmatrix}, \tag{11}$$

and λ_j is one of the (possible complex) eigenvalues of matrix $\boldsymbol{B}$. The first zero-eigenvalue is derived from the zero row-sums of matrix $\boldsymbol{B}$. By applying the change of variable $\xi = \boldsymbol{\delta}\boldsymbol{P}^{-\top}$, one obtains

$$\dot{\xi} = \boldsymbol{H}\xi + \varepsilon\boldsymbol{\Gamma}\xi\boldsymbol{J}^{\top}. \tag{12}$$

Each block of the Jordan canonical form corresponds to a subset of equations in Eq. (12). For the first block, the zero solution is asymptotically stable because $\boldsymbol{H}$ is a Hurwitz matrix. Then we take the mth block as an example. If the L_m is $k\times k$ in dimension, then it takes the form

$$\dot{\xi_1} = [\boldsymbol{H} + \rho\boldsymbol{\Gamma}]\xi_1, \tag{13}$$

$$\dot{\xi_2} = [\boldsymbol{H} + \rho\boldsymbol{\Gamma}]\xi_2 + \rho\boldsymbol{\Gamma}\xi_1, \tag{14}$$

$$\vdots \tag{15}$$

$$\dot{\xi_k} = [\boldsymbol{H} + \rho\boldsymbol{\Gamma}]\xi_k + \rho\boldsymbol{\Gamma}\xi_{k-1}, \tag{16}$$

where $\rho = \varepsilon\lambda_m$ and $\xi_1, \xi_2, \ldots, \xi_k$ are errors in the generalized eigenspace of eigenvalue λ_m of matrix $\boldsymbol{B}$.

Consider the stability of ξ_1, first, and take the Lyapunov function

$$V = \xi_1^{\top}\bar{\xi_1}, \tag{17}$$

then the derivative of the Lyapunov function with respect to Eq. (13) will be

$$\begin{aligned}\dot{V} &= [\dot{\xi_1}^{\top}\bar{\xi_1} + \xi_1^{\top}\dot{\bar{\xi_1}}] \\ &= \xi_1^{\top}[(\boldsymbol{H}+\rho\boldsymbol{\Gamma})^{\top} + \overline{(\boldsymbol{H}+\rho\boldsymbol{\Gamma})}]\bar{\xi_1} \\ &= \xi_1^{\top}[(\boldsymbol{H}+\varepsilon(\mathrm{Re}(\lambda)+\mathrm{jIm}(\lambda))\boldsymbol{\Gamma})^{\top} \\ &\quad + \overline{(\boldsymbol{H}+\varepsilon(\mathrm{Re}(\lambda)+\mathrm{jIm}(\lambda))\boldsymbol{\Gamma})}]\bar{\xi_1} \\ &= \xi_1^{\top}[(\boldsymbol{H}+\varepsilon\mathrm{Re}(\lambda)\boldsymbol{\Gamma})^{\top} + (\boldsymbol{H}+\varepsilon\mathrm{Re}(\lambda)\boldsymbol{\Gamma})]\bar{\xi_1},\end{aligned} \tag{18}$$

where j is the imaginary unit.

If $(\boldsymbol{H}+\varsigma_m\boldsymbol{\Gamma})^{\top} + (\boldsymbol{H}+\varsigma_m\boldsymbol{\Gamma}) < 0$, where $\varsigma_m = \varepsilon\mathrm{Re}(\lambda_m)$, the zero solution of Eq. (13) is asymptotically stable, i.e., $\xi_1 \to 0$ exponentially as $t \to +\infty$.

As the norm of $\boldsymbol{\Gamma}$ is bounded, the second term on the right-hand side of Eq. (14) is exponentially small. Then the same condition $(\boldsymbol{H}+\varsigma_m\boldsymbol{\Gamma})^{\top}+(H+\varsigma_m\boldsymbol{\Gamma}) < 0$, now applied to Eq. (14), guarantees the stabilizing effect of both the first and the second terms, resulting in the exponential convergence $\xi_2 \to 0$ as $t \to +\infty$. The same argument applied repeatedly shows that $\xi_3, \ldots, \xi_k$ must also converge to zero if $(\boldsymbol{H}+\varsigma_m\boldsymbol{\Gamma})^{\top} + (H+\varsigma_m\boldsymbol{\Gamma}) < 0$. This shows that $(\boldsymbol{H}+\varsigma_m\boldsymbol{\Gamma})^{\top}+(\boldsymbol{H}+\varsigma_m\boldsymbol{\Gamma}) < 0$ is a necessary and sufficient condition for the linear stability of the equations corresponding to each full block L_j. This condition is valid not only in diagonalizable networks[20] but also in nondiagonalizable networks. Thus we obtain the following Proposition.

Proposition 2.1. The networks X and Y achieve synchronization if $(\boldsymbol{H}+\varsigma\boldsymbol{\Gamma})^{\top}+(\boldsymbol{H}+\varsigma\boldsymbol{\Gamma}) < 0$, where $\boldsymbol{H}$ is a Hurwitz matrix, $\varsigma = \varepsilon\mathrm{Re}(\lambda)$, and λ is the nonzero eigenvalue of matrix $\boldsymbol{B}$.

Remark: There is a crucial difference between the diagonalizable and the nondiagonalizable cases. If $\boldsymbol{B}$ is diagonalizable, then all Jordan blocks are 1×1 in dimension, so there would be no equations like Eq. (14) or Eq. (16), and each error is decoupled from the others. Thus, the exponential convergence occurs independently and simultaneously. On the other hand, if $\boldsymbol{B}$ is not diagonalizable, some errors may suffer a long transient.

3. Synchronization between different motifs

There are 13 types of three-node motifs (see Fig. 1) and 169 four-node motifs[3] (see Fig. 2). Taking these motifs as the basic elements, one can synthesize many kinds of complex networks. So it is important to study the synchronization between different motifs. In this section, we will study the synchronization between different motifs with the theoretical results of last section in a numerical way.

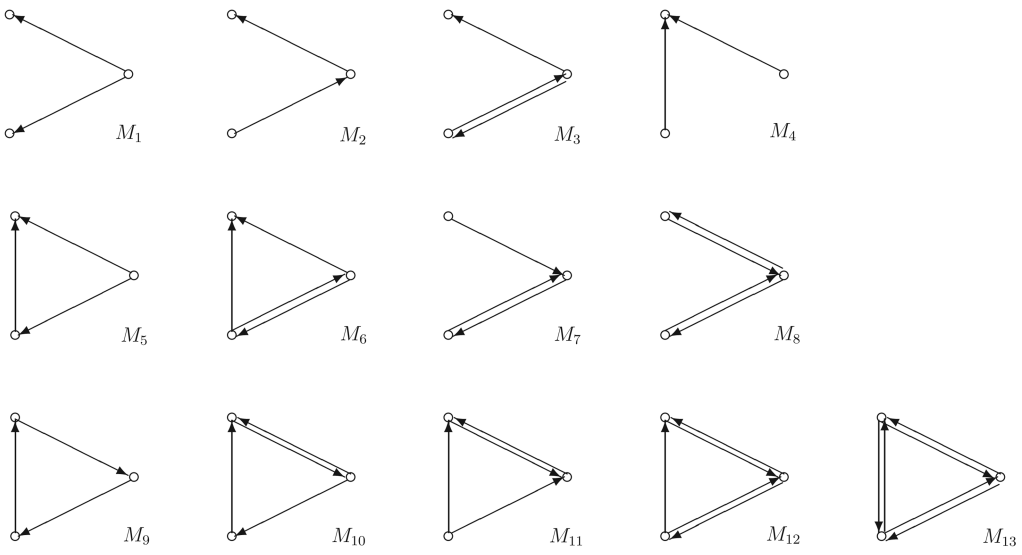


Fig. 1. Three-node motifs.

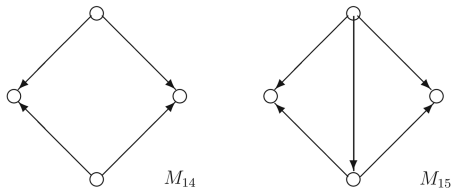


Fig. 2. Two of 169 four-node motifs.

In order to show the difference between motifs, we take several representative examples with different topological structures and different dynamical behaviours. For example, motifs M_9 and M_5 have different topological structures with different connections between nodes; motifs M_9 and M_{15} with different numbers of nodes and different connections between nodes. For the different dynamical behaviours of motifs, we use the familiar Lorenz system and two other chaotic systems of the Sprott's collection[18,24] to describe the dynamics of motifs M_9 and M_5, M_{15} respectively. Chaos is now thought to be rather common in nature and the dynamical behaviours of many kinds of real systems can be described by chaotic systems. So here, we choose the chaotic systems to describe the dynamics of motifs' nodes. Other dynamical systems can also be used and the conditions of synchronization can also be obtained similarly.

In the following, we take two three-node motifs and one four-node motif as examples and give the conditions for them to achieve synchronization. The synchronization of other motifs(including three- or four- and even five-node motifs) can be achieved similarly. Thus the synchronization of the whole network synthesized by motifs can be easily achieved.

Taking M_9 as the driving network, M_5 and M_{15} as the responding networks, respectively. By these examples, we show that the synchronization can be reached between networks with the same numbers of nodes or networks with different numbers of nodes. In M_9, the dynamics of individual node is described by Lorenz system which is coupled by the first variable as follows:

$$\begin{aligned}
\dot{x}_{i1} &= \sigma(x_{i2} - x_{i1}) + \mu \sum_{j=1}^{3} a_{ij} x_{j1}, \\
\dot{x}_{i2} &= r x_{i1} - x_{i1} x_{i3} - x_{i2}, \\
\dot{x}_{i3} &= x_{i1} x_{i2} - b x_{i3}, \ i = 1, 2, 3,
\end{aligned} \tag{19}$$

where $\sigma = 10$, $r = 28$, $b = 8/3$, and the coupling matrix is

$$\boldsymbol{A} = \begin{pmatrix} -1 & 0 & 1 \\ 1 & -1 & 0 \\ 0 & 1 & -1 \end{pmatrix}.$$

The individual uncoupled Lorenz system($\mu \equiv 0$) is eventually dissipative.[21] From Refs. [21] and [22], we know that M_9 achieves the synchronization when

$$\mu > 2 \times \frac{c}{3} > \frac{2}{3}\left(\frac{b(b+1)(r+\sigma)^2}{16(b-1)} - \sigma\right) = 32.56.$$

When $\mu = 38$, Fig. 3 indicates the time evolution of errors, showing the synchronization within motif M_9. The synchronization manifold is described as follows:

$$\begin{aligned}
\dot{x}_1 &= \sigma(x_2 - x_1), \\
\dot{x}_2 &= r x_1 - x_1 x_3 - x_2, \\
\dot{x}_3 &= x_1 x_2 - b x_3,
\end{aligned} \tag{20}$$

where σ, r, and b have been defined above. Figure 4 gives the time evolution of Lerens system (20).

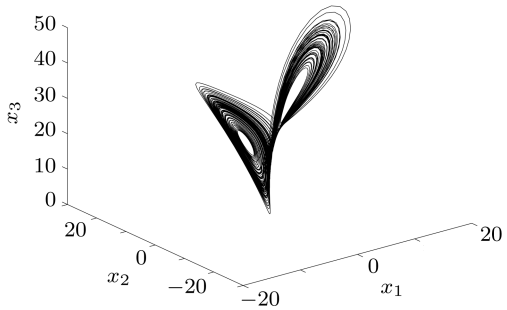


Fig. 3. Lorenz system (20).

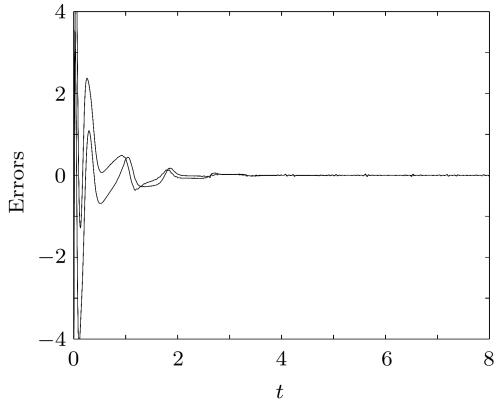


Fig. 4. Time evolutions of errors $x_{11} - x_{21}$ and $x_{11} - x_{31}$ of system (19) with $\mu = 38$.

In motif M_5, we use one of the chaotic systems of Sprott's collection[18,24] to describe the dynamics of uncoupled individual nodes without driving as follows:

$$\dot{y}_{i1} = y_{i2} y_{i3},$$

$$\dot{y}_{i2} = y_{i1} - y_{i2},$$
$$\dot{y}_{i3} = 1 - y_{i1}^2,\ i = 1, 2, 3. \tag{21}$$

Figure 5 gives the time evolution of system (21).

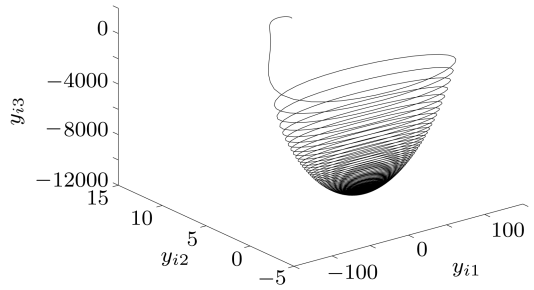


Fig. 5. Chaotic system (21).

The coupling matrix of motif M_5 is

$$\boldsymbol{B} = \begin{pmatrix} 0 & 0 & 0 \\ 1 & -1 & 0 \\ 1 & 1 & -2 \end{pmatrix},$$

the eigenvalues of which are $\lambda = 0,\ -1,\ -2$.

Here we set $\boldsymbol{\Gamma} = \mathrm{diag}(1, 0, 1)$ and $\boldsymbol{H}$ to be in the following form:

$$\boldsymbol{H} = \begin{pmatrix} 0 & p & -1 \\ 1 & -1 & 0 \\ 1 & 0 & 0 \end{pmatrix},$$

where p is a parameter. When $p < 0$, $\boldsymbol{H}$ is a Hurwitz matrix.[18]

It is easy to find that when $(p + 1)^2 < 4\varepsilon$, $(\boldsymbol{H} + \varsigma\boldsymbol{\Gamma})^\top + (\boldsymbol{H} + \varsigma\boldsymbol{\Gamma}) < 0$ holds. Figure 6 gives the time evolution of errors with $p = -1$ and $\varepsilon = 1$, which illuminates the synchronization between motifs M_9 and M_5.

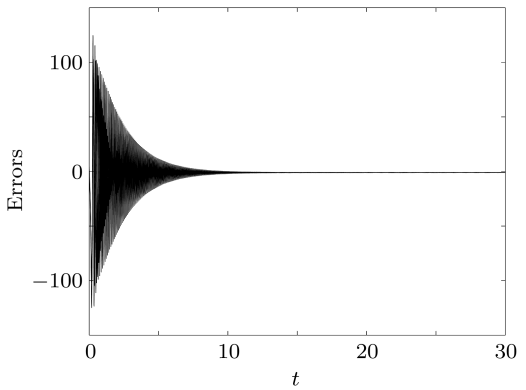


Fig. 6. Time evolutions of errors $x_1 - y_{i1},\ i = 1, 2, 3$, between motifs M_9 and M_5, with $p = -1$, $\varepsilon = 1$.

In motif M_{15}, the dynamics of uncoupled individual nodes without driving is described as follows:

$$\dot{y}_{i1} = -2y_{i2},$$
$$\dot{y}_{i2} = y_{i1} + y_{i3}^2,$$
$$\dot{y}_{i3} = 1 + y_{i2} - 2y_{i3},\ i = 1, 2, 3, 4. \tag{22}$$

Figures 7 gives the time evolution of system (22).

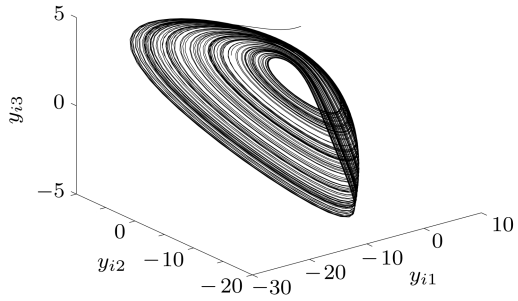


Fig. 7. Chaotic system (22).

The coupling matrix of motif M_{15} is

$$\boldsymbol{B} = \begin{pmatrix} 0 & 0 & 0 & 0 \\ 1 & -1 & 0 & 0 \\ 1 & 1 & -2 & 0 \\ 1 & 1 & 0 & -2 \end{pmatrix},$$

the eigenvalues of which are $\lambda = 0, -1, -2, -2$.

Set $\boldsymbol{\Gamma} = \mathrm{diag}(1, 1, 0)$ and

$$\boldsymbol{H} = \begin{pmatrix} 0 & -2 & 0 \\ 1 & 0 & p \\ 0 & 1 & -2 \end{pmatrix},$$

where p is a parameter. When $p < 0$, $\boldsymbol{H}$ is a Hurwitz matrix.[18]

It is easy to verify that when $p = -1$ and $\varepsilon > 0.5$, $(\boldsymbol{H} + \varsigma\boldsymbol{\Gamma})^\top + (\boldsymbol{H} + \varsigma\boldsymbol{\Gamma}) < 0$ holds. Figure 8 shows the time evolution of errors with $p = -1$ and $\varepsilon = 1$, illuminating the synchronization between motifs M_9 and M_{15}.

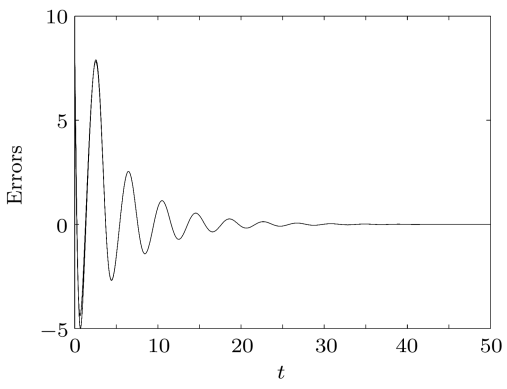


Fig. 8. Time evolutions of errors $x_1 - y_{i1},\ i = 1, 2, 3, 4$, between motifs M_9 and M_{15}, with $p = -1$, $\varepsilon = 1$.

4. Conclusions and discussion

In this paper, we give the method and conditions to achieve the synchronization between different motifs. In order to study the synchronization between different motifs, we have first studied the synchronization between two networks with different topology structures and different dynamical behaviours. Specifically, under the precondition that the driving network achieves the synchronization, we obtain the conditions for the synchronization between two different networks by using the OPCL method. Then, taking three-node and four-node motifs, the basic elements for synthesizing networks, as examples we study the synchronization between different motifs which verifies the effectiveness and the feasibility of the synchronization scheme.

Here, the two networks are taken as driving and responding systems respectively. After synchronization, the responding system has the same dynamical behaviour as the driving system. In other words, after synchronization, the nodes in two different motifs have the same dynamic behaviours as those in one of the original motifs. However, in many practical networks, some new dynamical behaviours are often required after synchronization. For example, in society networks, individual groups study merits from each other and avoid shortcomings of each other, and make a new progress together. This practical problem is reduced into the synchronous state which is different from any of the original states. In our further work, we will study the case that after synchronization of two different networks, a new dynamical behaviour different from those of the original networks emerges.

References

[1] Strogatz S H 2001 *Nature* (London) **410** 268
[2] Shen-Orr S, Milo R, Mangan S and Alon U 2002 *Nat. Genet.* **31** 64
[3] Milo R, Shen-Orr S and Itzkovitz S 2002 *Science* **298** 824
[4] Gao L F, Liu X and Guan S 2008 *Chin. Phys.* B **17** 4396
[5] Li Y, Liu Z R and Zhang J B 2007 *Chin. Phys.* **16** 2587
[6] Moreno Y, Vázquez-Prada M and Pacheco A F 2004 *Phys.* A **343** 279
[7] Wuchty S, Olivai Z N and Barabási A L 2003 *Nat. Genet.* **35** 176
[8] Lodato I, Boccaletti S and Latora V 2007 *Europhys. Lett.* **78** 28001
[9] Mangan S and Alon U 2003 *PNAS* **100** 11980
[10] Li C G, Chen L N and Aihara K 2007 *Signal Processing Magazine, IEEE* **24** 136
[11] Pecora L M and Carroll T L 1990 *Phys. Rev. Lett.* **64** 821
[12] Kocarev L and Parlitz U 1996 *Phys. Rev. Lett.* **76** 1816
[13] Ma Z J, Liu Z R and Zhang G 2006 *Chaos* **16** 023103
[14] Li Y, Liu Z R and Zhang J B 2008 *Chin. Phys. Lett.* **25** 874
[15] Li C P, Sun W G and Kurths J 2007 *Phys. Rev.* E **76** 046204
[16] Jackson E A and Grosu I 1995 *Phys.* D **85** 1
[17] Grosu I 1997 *Phys. Rev.* E **56** 3709
[18] Lerescu A I, Constandache N, Oancea S and Grosu I 2004 *Chaos, Solitons and Fractals* **22** 599
[19] Wang X F and Chen G 2002 *Int. J. Bifurcation Chaos Appl. Sci. Eng.* **12** 885
[20] Pecora L M and Carroll T L 1998 *Phys. Rev. Lett.* **80** 2109
[21] Belykh V N, Belykh I V and Hasler M 2004 *Phys.* D **195** 159
[22] Belykh I V, Belykh V N and Hasler M 2006 *Chaos* **16** 015102
[23] Nishikawa T and Motter A E 2006 *Phys. Rev.* E **73** 065106(R)
[24] Sprott J C 1994 *Phys. Rev.* E **55** 5285